Original Article

The transition from hypertension to hypertensive heart disease and heart failure with preserved ejection fraction: a retrospective cross-sectional study of myocardial magnetic resonance strain and tissue characteristics

Rui Li[1], Feng Lei[1], Feng Liu[1], Liang Cao[3], Xu Cao[2], Meng Niu[3], Shunlin Guo[3]

[1]Department of Radiology, The First Clinical Medical College, Lanzhou University, Lanzhou, China; [2]Department of Pulmonology, Baiyin Central Hospital of Gansu Province, Baiyin, China; [3]Department of Radiology, The First Hospital of Lanzhou University, Lanzhou, China

Contributions: (I) Conception and design: R Li; (II) Administrative support: S Guo; (III) Provision of study materials or patients: R Li, F Lei; (IV) Collection and assembly of data: R Li, F Lei, M Niu; (V) Data analysis and interpretation: F Liu, L Cao, X Cao, M Niu; (VI) Manuscript writing: All authors; (VII) Final approval of manuscript: All authors.

Correspondence to: Shunlin Guo, PhD; Meng Niu, MD. Department of Radiology, The First Hospital of Lanzhou University, Donggang West Road, Lanzhou 730000, China. Email: guoshunlin@msn.com; nium09@lzu.edu.cn.

Background: Due to the variability of symptoms and signs associated with heart failure, along with the lack of specific tests for definitive diagnosis, the noninvasive diagnosis of heart failure with preserved ejection fraction (HFpEF) continues to pose significant clinical challenges. This investigation was designed to elucidate the clinical manifestations of HFpEF and to analyze cardiac magnetic resonance (CMR)-derived myocardial strain metrics and tissue characteristics in a cohort exhibiting HFpEF with hypertension (HFpEF-HTN).

Methods: This retrospective analysis consisted of 128 patients diagnosed HFpEF-HTN, 78 individuals with hypertensive heart disease (HHD), 89 individuals with hypertension (HTN), and 60 normotensive healthy controls and was conducted from August 2021 to February 2024. All participants were recruited from The First Hospital of Lanzhou University and underwent laboratory examinations and 3.0 T CMR. The study compared clinical features and CMR-derived structural and functional parameters across different groups. Logistic regression was employed to determine the association between CMR parameters and HFpEF-HTN. Spearman correlation coefficient analysis was used to clarify the relationship between myocardial strain parameters and left ventricular (LV) ejection fraction and right ventricular (RV) ejection fraction. Additionally, the area under the curve (AUC) from receiver operating characteristic (ROC) analysis was used to compare the diagnostic performance of different CMR parameters for HFpEF-HTN.

Results: Patients diagnosed with (HFpEF-HTN) were characterized by an older demographic profile, a higher prevalence of smoking history, elevated systolic and diastolic blood pressure, increased levels of N-terminal pro-brain natriuretic peptide, and more advanced New York Heart Association functional class as compared to other studied groups. In terms of myocardial deformation, individuals with HFpEF-HTN exhibited pronounced impairments in both LV and RV function, as evidenced by significantly reduced longitudinal strain (LS), circumferential strain (CS), and radial strain (RS), relative to HTN, HHD, the control cohorts (all P values <0.001). Patients with HFpEF-HTN showed significantly elevated levels of late gadolinium enhancement, native T1, and extracellular volume fraction (ECV) indicative of myocardial interstitial fibrosis as compared to patients with HHD. Additionally, as compared to ECV, LV GCS emerged as a superior diagnostic indicator, demonstrating greater diagnostic accuracy in differentiating HFpEF-HTN

patients from those with HHD (AUC =0.85; P<0.001). Moreover, LVEF showed a mild correlation with CMR-derived LV GLS (R=–0.43; P<0.001), LV GCS (R=–0.42; P<0.001), and LV GRS, (R=0.56; P<0.001) in all patients.

Conclusions: Myocardial strain, T1 mapping, and ECV can be used for the quantitative evaluation of LV and RV ventricular remodeling, dysfunction, and tissue characteristics in patients with HFpEF-HTN and thus hold significant potential for the diagnosis of these patients.

Keywords: Heart failure with preserved ejection fraction (HFpEF); cardiovascular magnetic resonance (CMR); myocardial strain; T1mapping; extracellular volume

Submitted Apr 21, 2024. Accepted for publication Aug 26, 2024. Published online Sep 26, 2024.
doi: 10.21037/qims-24-803
View this article at: https://dx.doi.org/10.21037/qims-24-803

Introduction

Hypertension (HTN) poses a significant public health challenge worldwide, with its prevalence increasing in China due to urbanization, rising incomes, and an aging population (1-3). HTN survey of China conducted from 2012 to 2015 revealed that approximately 23.2% of Chinese adults aged years 18 and above, equivalent to around 244.5 million individuals, were affected by HTN (4). HTN is a major risk factor for incident heart failure (HF), particularly in heart failure with preserved ejection fraction (HFpEF), which is more prevalent compared to HF with reduced ejection fraction (HFrEF) (5). In patients with established HFpEF, HTN is present in 90% of cases (6). However, differentiating HFpEF-HTN from HTN and hypertensive heart disease (HHD) based on noninvasive imaging is challenging due to the subtle cardiac dysfunction and subclinical changes in myocardial structure that these patients share (7).

Cardiac magnetic resonance (CMR) imaging has emerged as the gold standard for the noninvasive assessment of cardiac morphology and function, especially through advanced techniques such as CMR feature tracking (CMR-FT) and extracellular volume fraction (ECV) (8). These tools facilitate the detection of subtle cardiac dysfunction and subclinical changes using strain parameters and tissue characteristics (7,9). One study demonstrated the prognostic value of CMR-FT-derived strain parameters and ECV across the spectrum of HFpEF (10). However, there is a scarcity of studies that have investigated cardiac dysfunction based on CMR-FT, T1 mapping, and ECV in patients with both the HFpEF and HTN phenotype (HFpEF-HTN) as compared to their general HFpEF counterparts. Therefore, this study aimed to investigate the clinical features and CMR-derived LV and right ventricular (RV) remodeling, dysfunction, and tissue characteristics in patients with HFpEF-HTN. Additionally, it sought to quantify these phenotypically diverse patients in comparison to individuals with HHD, HTN, and healthy controls. We present this article in accordance with the STROBE reporting checklist (available at https://qims.amegroups.com/article/view/10.21037/qims-24-803/rc).

Methods

Study population

In this retrospective cross-sectional study, 295 consecutive patients and 60 healthy individuals who underwent CMR between August 2021 and February 2024 were recruited from The First Hospital of Lanzhou University. Eligible participants were categorized into the HFpEF-HTN group if they met the following criteria: (I) clinical diagnosis of HTN; (II) presentation of typical HF symptoms, such as palpitations, anxiety, chest congestion, and exercise intolerance corresponding to New York Heart Association (NYHA) functional classes II–IV; (III) preserved LVEF >50% on echocardiography; and (IV) a score of ≥5 according to the heart failure association-pre-test assessment, echocardiography and natriuretic peptide score, functional testing in cases of uncertainty, final aetiology (HFA-PEFF) algorithm, which incorporates echocardiographic data, brain natriuretic peptide (BNP) levels, functional testing in cases of uncertainty, and a final assessment of etiology (11). HHD was defined as increased LV wall thickness (≥12 mm) in the presence of arterial HTN without other cardiac or systemic diseases (12). Participants were classified as having HHD if their LV mass index (LVMI)

exceeded 5 standard deviations (SDs) above the mean for the Chinese population on 3-T magnetic resonance imaging (MRI) (>81 g/m^2 for men or >62 g/m^2 for women) (13,14). HTN was defined as an office systolic blood pressure (SBP) of ≥140 mmHg and/or a diastolic blood pressure (DBP) of ≥90 mmHg (15). Exclusion criteria for the study included secondary HTN, underlying cardiomyopathies (such as hypertrophic cardiomyopathy, dilated cardiomyopathy, restrictive cardiomyopathy and cardiac amyloidosis), ischemic heart disease, severe arrhythmias, significant valvular heart disease, anemia, hyperthyroidism, and a history of myocardial infarction or heart surgery. Healthy individuals without apparent structural heart disease on CMR were included as the control group. This study was conducted in accordance with the Declaration of Helsinki (as revised in 2013) and was approved by the Ethics Committee of The First Hospital of Lanzhou University (No. LDYYLL-2024-470). The requirement for individual consent was waived due to the retrospective nature of the analysis.

CMR scanning protocol

MRI was performed in a 3-T scanner (Philips Healthcare, Amsterdam, the Netherlands). LV and RV function cine images were acquired using a breath-hold balanced steady-state free precession (bSSFP) sequence with retrospective electrocardiogram (ECG) gating in long-axis planes (2-, 3-, and 4-chamber views) and contiguous short-axis slices covering both ventricles. The typical cine imaging parameters were as follows: repetition time (TR)/echo time (TE), 3.0 ms/1.1 ms; flip angle, 65–85°; matrix size, 256×113; field of view (FOV), 340 mm × 280 mm; and slice thickness, 6–8 mm.

Native T1 mapping

A modified Look-Locker inversion recovery (MOLLI) sequence was used for T1 mapping (16). The MOLLI sequence was performed in the LV short axis for all patients, targeting the base, midchamber, and apex. The standard imaging parameters for the T1 map included a matrix size of 162×256, a slice thickness of 10 mm, and TR/TE values of 2.5/1.0 ms.

Late gadolinium enhancement (LGE) imaging

LGE imaging was performed in the same image planes approximately 10–15 minutes after administration of 0.15 mmol/kg of body weight of gadobutrol (Bayer AG, Leverkusen, Germany). A middiastolic inversion-prepared two-dimensional (2D) gradient echo sequence was used with the following parameters: TE/TR, 1.7 ms/3.3 ms; flip angle, 25°; matrix size, 188×158, FOV, 300 mm × 300 mm; interpolated voxel size, 1.6×1.9×10 mm; segmented breath-hold sequence; and an acquisition window positioned within the cardiac cycle at end-diastole.

Postprocessing

LV and RV morphology and function measurement

Cardiac structure and functional deformation were measured semiautomatically using specialized CMR software (CVI42 version 5.9.3, Circle Cardiovascular Imaging, Calgary, Canada), initiated by an automated contour algorithm. Two observers, each with two years of experience using the software, conducted the assessment. Standard parameters of cardiac structure, including indexed ventricular volumes and mass relative to body surface area, and ejection fraction were evaluated.

MR feature tracking

For strain analysis, the endocardial and epicardial contours were automatically identified with manual adjustments made at end-systole and end-diastole using CVI42 in 2D long-axis and short-axis stacks. The endocardial contour specifically excluded the papillary muscles (*Figure 1*).

Native T1 and ECV measurement

The native T1 measurement was conducted using CVI42. The native T1 values were assessed in the myocardium across all three slices from the base to the apex with no exclusion of the LGE scar. The calculation of ECV values with red blood cell volume correction was performed via contour measurements on pre- and postcontrast T1 mapping in the endocardium and epicardium (*Figure 1*).

LGE image interpretation

Quantification of LGE was performed using the full width at half maximum method according to the following formula: LGE volume fraction = LGE myocardial volumetotal myocardial volume.

Data reproducibility

The intra- and interobserver variability of each CMR strain parameter was evaluated in terms of intraclass correlation

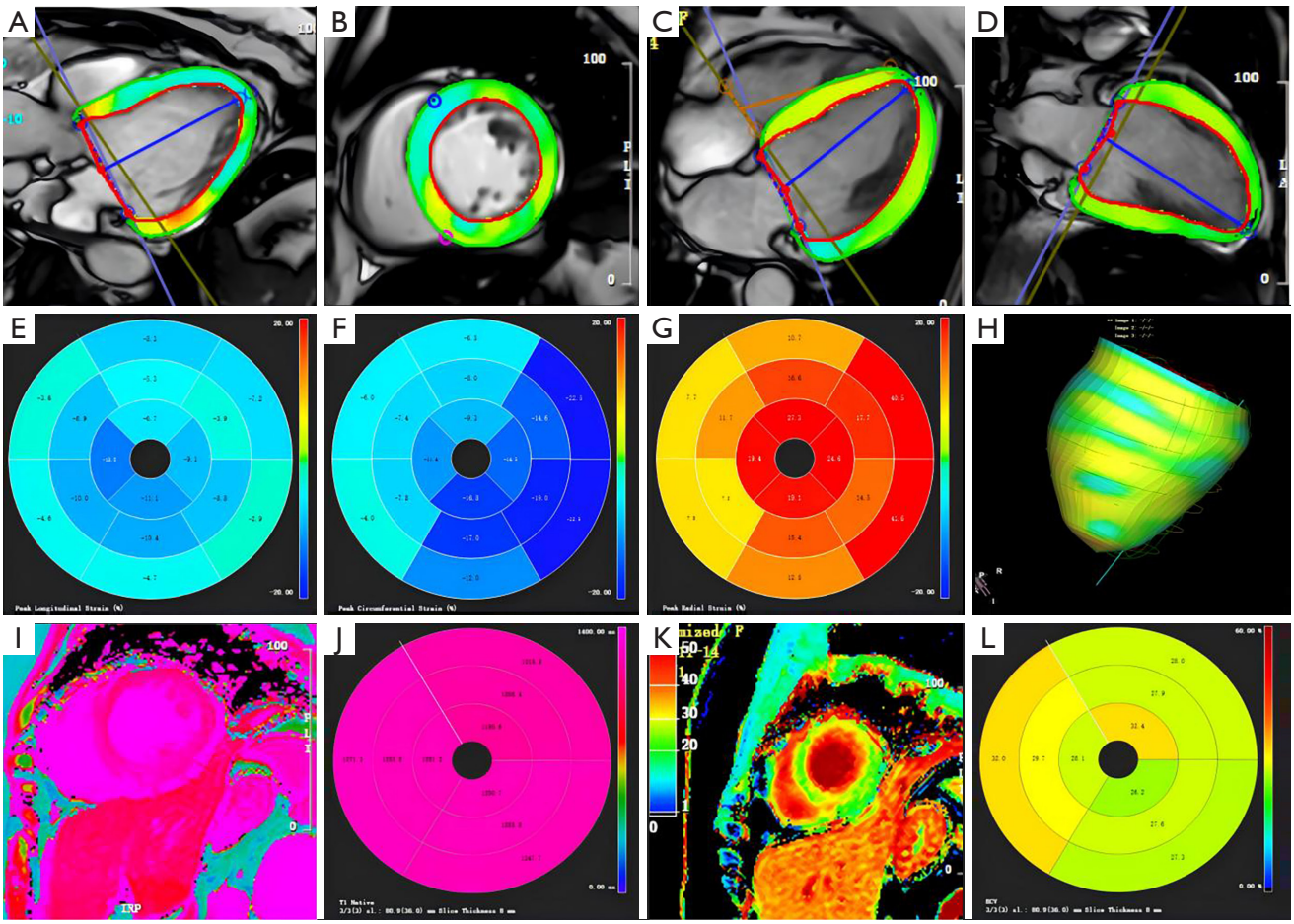

Figure 1 Feature tracking, T1 mapping, and ECV analysis performed on routine cardiac cine images. (A-D) In both long-axis and short-axis views, the endocardial and epicardial contours were automatically detected, with manual corrections applied as needed. (E-G) Deeper shades of red and blue indicated poorer heart function of the LV. (H) Three-dimensional model of the LV myocardium. (I-K) Schematic diagram and value of T1 mapping and ECV. ECV, extracellular volume; LV, left ventricular.

coefficient (ICC) in a subset of 25 randomly selected patients. Two radiologists who were blinded to the clinical information of the patients performed the assessments.

Statistical analysis

We examined the normality of continuous data and present the continuous variables as the mean ± SD and the categorical variables as frequency (percentage). Group comparisons were performed using one-way analysis of variance (ANOVA) and two-sample *t*-tests or Mann-Whitney tests with by Bonferroni post hoc correction. Continuous variables were examined using scatterplots and Pearson correlation coefficient (R). Logistic regression was employed to investigate the association between CMR parameters and HFpEF-HTN. Additionally, receiver operating characteristic (ROC) curve analysis was used to determine which parameters could effectively distinguished the HFpEF-HTN group from the HHD group and the HTN group from healthy controls. A two-sided P value <0.05 was regarded as indicating a statistically significant difference.

Results

Baseline data

Our study consecutively enrolled 128 patients with HFpEF-HTN, 78 patients with HHD, 89 patients with only pure HTN, and 60 controls. The reasons for exclusion and

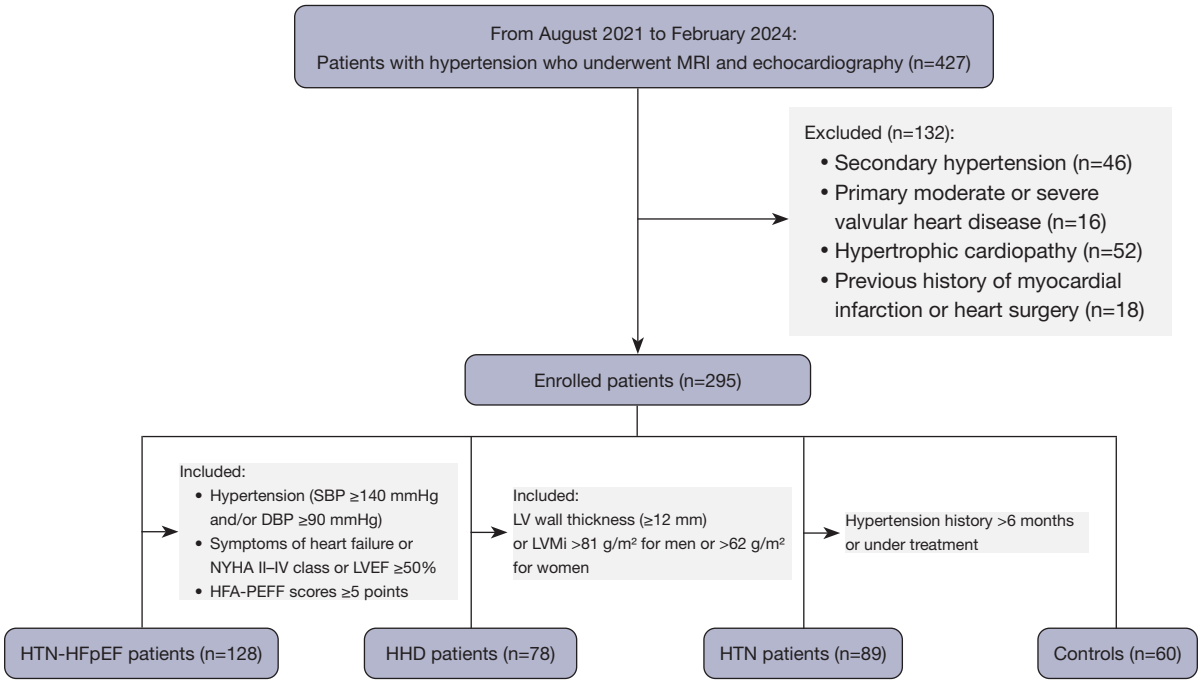

Figure 2 Patient flowchart. MRI, magnetic resonance imaging; SBP, systolic blood pressure; DBP, diastolic blood pressure; NYHA, New York Heart Association; LVEF, left ventricular ejection fraction; HFA-PEFF, heart failure association-pre-test assessment, echocardiography and natriuretic peptide score, functional testing in cases of uncertainty, final aetiology; LV, left ventricular; LVMi, LV mass index; HTN, hypertension; HFpEF, heart failure with preserved ejection fraction; HHD, hypertensive heart disease.

baseline data are shown in *Figure 2* and *Table 1*, respectively. No significant differences were observed in terms of gender, creatinine levels, or drug usage between the four groups (all P values >0.05). Compared to patients in the other groups, those in the HFpEF-HTN group were more likely to be older; have a history of smoking; have elevated systolic BP, diastolic BP, NT-proBNP levels; and have a higher NYHA functional class. In comparison to patients with HTN, patients with HHD exhibited higher NT-proBNP levels but lower NYHA class I/II.

CMR baseline data

There were no statistically significant differences in heart rate, LVEF, RVEF, or cardiac index between the groups (all P values >0.05). The HFpEF-HTN group exhibited higher LV and RV end-diastolic volume index (EDVi), end-systolic volume index (ESVi), LV maximum wall thickness, and LVMi compared to the HTN and HHD groups (P<0.001), indicating more severe LV and RV remodeling (*Table 2*). IN comparison to the respective reference values, MRI and echocardiography examinations revealed no signs of cardiac dysfunction in healthy controls.

CMR strain imaging parameters and identification of HFpEF-HTN

Regarding myocardial strain, patients with HFpEF-HTN exhibited more severe LV and RV dysfunction, with LV and RV longitudinal strain (LS), circumferential strain (CS), and radial strain (RS) being significantly decreased as compared to those in the HTN, HHD, and control groups (all P values <0.001) (*Figure 3*, *Table 2*).

Myocardial tissue characteristics derived from CMR LGE, T1 mapping, and ECV

Compared to patients with HHD, patients with HFpEF-HTN showed significantly elevated levels of LGE, native T1, and ECV, indicating myocardial interstitial fibrosis

Table 1 Baseline characteristics

Variables	HFpEF-HTN (n=128)	HHD (n=78)	HTN (n=89)	Controls (n=60)	P
Age (years)	60±12*#†	56±10#†	49±11†	42±12	<0.001
Male (%)	80 (62.5)	43 (55.0)	50 (56.1)	27 (45.0)	0.062
Smoking history (%)	42 (32.8)*#†	20 (25.6)#†	20 (22.5)†	10 (16.7)	<0.001
Systolic BP (mmHg)	163±21*#†	159±18†	156±17†	111±13	<0.001
Diastolic BP (mmHg)	99±17*#†	98±16#†	93±12†	72±10	<0.001
NT-proBNP (pg/mL)	300 [232–812]*#†	106 [89–115]#†	87 [43–106]†	37 [26–45]	<0.001
NYHA class I/II (%)	83 (64.8)*#	70 (89.7)#†	89 (100.0)	–	<0.001
NYHA class III/IV (%)	45 (35.2)*#	8 (10.3)#†	0	–	<0.001
Creatinine (μmol/L)	95.6±16.3	92.3±18.9	90.3±11.6	75.8±13.7	0.241
Triglyceride (mmol/L)	1.9±1.0#†	1.7±1.2#†	1.4±0.6†	1.2±0.3	0.046
Hemoglobin (g/L)	146±18#†	143±14#†	140±17†	135±15	<0.001
ACEI/ARB (%)	100 (78.1)	58 (74.4)	49 (55.1)	–	0.064
β-blocker (%)	104 (81.3)	62 (79.5)	63 (70.8)	–	0.088
Statin (%)	85 (66.4)	47 (60.3)	46 (51.7)	–	0.051
Aspirin (%)	90 (70.3)	55 (70.5)	49 (54.9)	–	0.213
Diuretic (%)	82 (64.1)	45 (57.7)	45 (50.6)	–	0.102

Values are given as the mean ± standard deviation, as medians [interquartile range], or as percentages. *, P<0.05 *vs.* HHD; #, P<0.05 *vs.* HTN; †, P<0.05 *vs.* controls. HFpEF, heart failure with preserved ejection fraction; HTN, hypertension; HHD, hypertensive heart disease; BP, blood pressure; NT-proBNP, N-terminal pro-brain natriuretic peptide; NYHA, New York Heart Association; ACEI/ARB, angiotensin-converting enzyme inhibitors/angiotensin receptor blockers.

(*Figure 4*, *Table 2*).

Correlation between myocardial strain parameters and LVEF and RVEF parameters

Among the four groups, moderate correlations were observed between several FT-derived strain parameters and RVEF (RV GLS: R=–0.42; RV GCS, R=–0.55; RV GRS: R=0.58, all P values <0.001). LVEF showed a mild correlation with CMR-derived LV GLS (R=–0.43; P<0.001), LV GCS (R=–0.42; P<0.001), and LV GRS, (R=0.56, P<0.001) in all patients (*Figure 5*).

Identification of HFpEF-HTN

Logistic regression analysis was conducted specifically for patients with HFpEF-HTN and HHD. LV GRS, LV GCS, LV GLS, RV GRS, RV GCS, RV GLS, native T1, and ECV were significantly correlated with the diagnosis of HFpEF-HTN. In the multivariable logistic regression analysis involving these variables, LV GCS, RV GRS, RV GCS, RV GLS, native T1, and ECV were independently associated with the diagnosis of HFpEF-HTN (*Table 3*). According to ROC curve analysis, LV GCS exhibited superior diagnostic ability in distinguishing patients with HFpEF-HTN from those with HHD, with an area under the curve (AUC) of 0.85 (95% CI: 0.79–0.91; P<0.001), which was greater than that of ECV (AUC =0.84; 95% CI: 0.78–0.89; P<0.001). Additionally, RV GCS proved to be a better at discriminating between patients with HTN and controls (AUC =0.88; 95% CI: 0.82–0.94; P<0.001). The optimal cutoff value for distinguishing between HFpEF-HTN and HHD using LV GCS was –14.49%, which yielded a sensitivity of 68% and a specificity of 89% (*Figure 6*).

Data reproducibility

All myocardial strain and tissue characteristic parameters demonstrated excellent intraobserver and interobserver consistency (ICC >0.85). Specifically, LV GRS showed

Table 2 CMR data

Variable	HFpEF-HTN (n=128)	HHD (n=78)	HTN (n=89)	Controls (n=60)	P
Heart rate (bpm)	72±15	69±14	73±18	71±13	0.06
Cardiac index (mL/m^2)	2.9±0.64	3.1±0.77	3.3±0.53	3.5±0.81	0.12
LVEF (%)	61.2±4.6	62.3±6.4	61.8±4.9	63.0±3.4	0.12
LVMWT (mm)	14.2±1.9$^{*\#\dagger}$	13.6±1.7$^{\#\dagger}$	11.2±1.4†	9.2±1.3	<0.001
LV EDVi (mL/m^2)	79.2±32.3*†	57.8±15.9$^{\#\dagger}$	72.3±33.2†	69.0±15.7	<0.001
LV ESVi (mL/m^2)	54.7±14.8$^{*\#\dagger}$	48.6±15.6†	47.3±11.2†	24.9±9.8	<0.001
LVMi (g/m^2)	60.0±20.4$^{*\#\dagger}$	52.6±14.6$^{\#\dagger}$	56.5±9.0†	43.1±11.5	<0.001
RVEF (%)	53.6±10.6	56.9±8.2	56.2±11.5	55.5±9.5	0.88
RV EDVi (mL/m^2)	68.5±14.3$^{*\#\dagger}$	49.9±16.1$^{\#\dagger}$	62.5±21.4†	64.4±17.6	<0.001
RV ESVi (mL/m^2)	42.6±12.6$^{*\#\dagger}$	33.8±10.6$^{\#\dagger}$	37.9±12.6†	35.6±13.9	<0.001
LV GRS (%)	24.4±4.1$^{*\#\dagger}$	26.6±3.4$^{\#\dagger}$	29.3±5.3†	33.2±3.6	<0.001
LV GCS (%)	−13.4±2.6$^{*\#\dagger}$	−15.8±2.7$^{\#\dagger}$	−18.3±3.4†	−19.1±1.8	<0.001
LV GLS (%)	−12.7±3.3$^{*\#\dagger}$	−13.6±2.2$^{\#\dagger}$	−16.6±1.8†	−18.2±2.2	<0.001
RV GRS (%)	22.3±3.6$^{*\#\dagger}$	25.5±7.5$^{\#\dagger}$	28.3±7.8†	31.6±5.0	<0.001
RV GCS (%)	−14.2±4.7$^{*\#\dagger}$	−16.5±2.7$^{\#\dagger}$	−18.7±3.2†	−21.3±3.6	<0.001
RV GLS (%)	−12.0±1.8$^{*\#\dagger}$	−13.2±3.1$^{\#\dagger}$	−15.1±2.8†	−18.7±2.5	<0.001
LGE percentage (%/LV)	1.75±0.39$^{*\#\dagger}$	1.25±0.19$^{\#\dagger}$	1.03±0.09	0	<0.001
Native T1 (ms)	1,365±116$^{*\#\dagger}$	1,216±110$^{\#\dagger}$	1,165±142†	1,087±98	0.016
ECV (%)	33.4±3.7$^{*\#\dagger}$	29.5± 3.6†	27.4±3.8†	25.3±4.1	0.003

Values are given as the mean ± standard deviation. *, P<0.05 *vs.* HHD; #, P<0.05 *vs.* HTN; †, P<0.05 *vs.* controls. CMR, cardiovascular magnetic resonance; HFpEF, heart failure with preserved ejection fraction; HTN, hypertension; HHD, hypertensive heart disease; LVEF, left ventricular ejection fraction; LVMWT, left ventricular maximum wall thickness; EDVi/ESVi, end-diastole/systole volume index; LVMi, left ventricular mass index; RVEF, right ventricular ejection fraction; GRS, global radial strain; GCS, global circumferential strain; GLS, global longitudinal; LGE, late gadolinium enhancement; LV, left ventricular; ECV, extracellular volume fraction.

excellent ICC for both intra- and interobserver consistency, with values exceeding 0.980 (*Table 4*).

Discussion

This study provide novel insights by offering detailed clinical and laboratory phenotyping, along with CMR strain and tissue characteristics, for the often underrepresented population of patients with HFpEF-HTN, with comparison to parameters of those with HHD and HTN and healthy controls. Our study produced several key findings: (I) both the HFpEF-HTN and HHD groups showed significant deterioration in systolic and diastolic properties compared to the HTN and control groups but showed no reduction in LVEF. (II) Patients with HFpEF-HTN exhibited further deterioration in systolic and diastolic properties compared to those with HHD. (III) LV GLS and RV GLS demonstrated a moderate correlation with LVEF and RVEF. (IV) ECV and native T1 were effective in identifying early-stage LV abnormalities in patients with HTN but not LGE, suggesting an increase in diffuse myocardial fibrosis to be associated with LV remodeling.

As a heterogeneous clinical syndrome characterized by complex pathophysiological features, HF represents the final stage of various cardiovascular diseases (17). This is especially notable in patients with HFpEF, in whom HTN emerges as the most prevalent and detrimental comorbidity (18,19). Even with recommended guidelines in place, diagnosing HFpEF continues to pose challenges (20,21). Recently, CMR-FT has shown promise in detecting

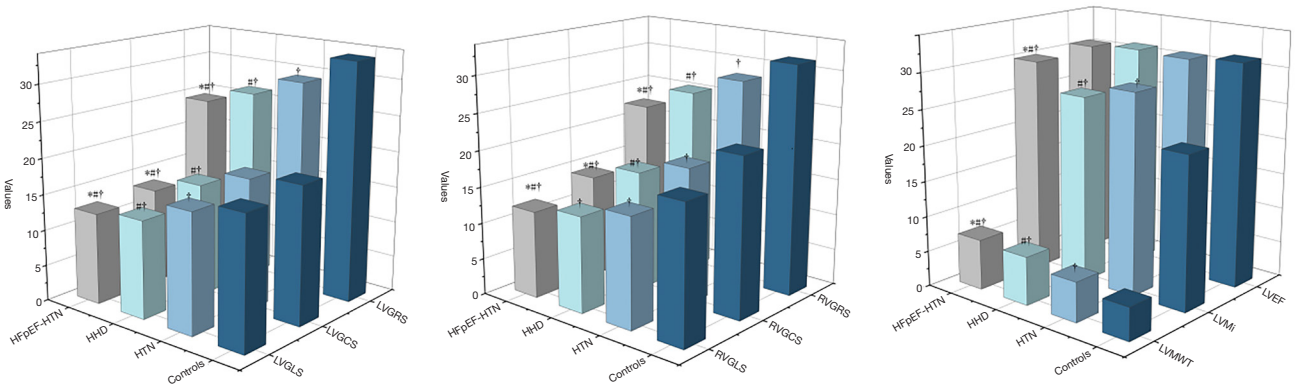

Figure 3 Comparison of the CMR parameters in the four groups. Data are presented as bar graphs showing the mean values. Strain parameters are expressed as absolute values, with lower values indicating worse cardiac function. *, P<0.05 *vs.* HHD; #, P<0.05 *vs.* HTN; †, P<0.05 *vs.* controls. HFpEF, heart failure with preserved ejection fraction; HTN, hypertension; HHD, hypertensive heart disease; LV, left ventricular; GRS, global radial strain; GCS, global circumferential strain; GLS, global longitudinal; RV, right ventricular; LVEF, left ventricular ejection fraction; LVMi, left ventricular mass index; LVMWT, left ventricular maximum wall thickness; CMR, cardiovascular magnetic resonance.

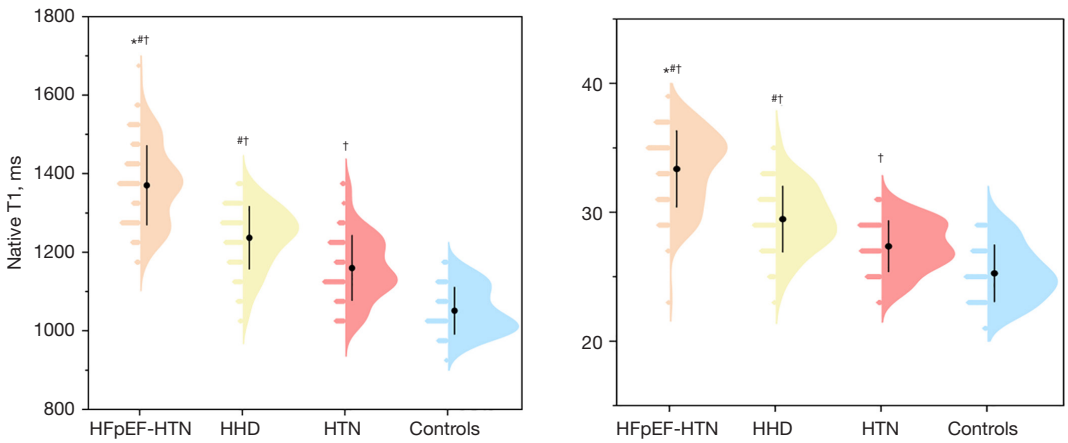

Figure 4 Half violin plots showing T1 mapping and ECV in the four groups. *, P<0.05 *vs.* HHD; #, P<0.05 *vs.* HTN; †, P<0.05 *vs.* controls. HFpEF, heart failure with preserved ejection fraction; HTN, hypertension; HHD, hypertensive heart disease; ECV, extracellular volume fraction.

subclinical myocardial damage earlier than EF, without requiring additional sequences or contrast medium. However, only a limited number of studies have examined the subtle LV functional differences between individuals with HFpEF-HTN, and HTN and healthy controls using CMR-FT strain analysis (7,22). The strengths of our present study are evident in our ability to showcase the detailed dynamic changes in LV and RV functional parameters as LV and RV diastolic dysfunction progressed. Furthermore, our findings indicate that CMR-derived LV and RV myocardial strain, in conjunction with tissue characteristics, may hold diagnostic value in individuals with HFpEF-HTN.

The study findings align with previous research supporting the value of BNP as a functional biomarker of HFpEF and its role as a prognostic indicator for hospitalization and mortality in patients with HFpEF (23,24). Moreover, our findings are consistent with those of a study by Mordi *et al.* (25), in which 62 patients with HFpEF were evaluated. It was found that these patients

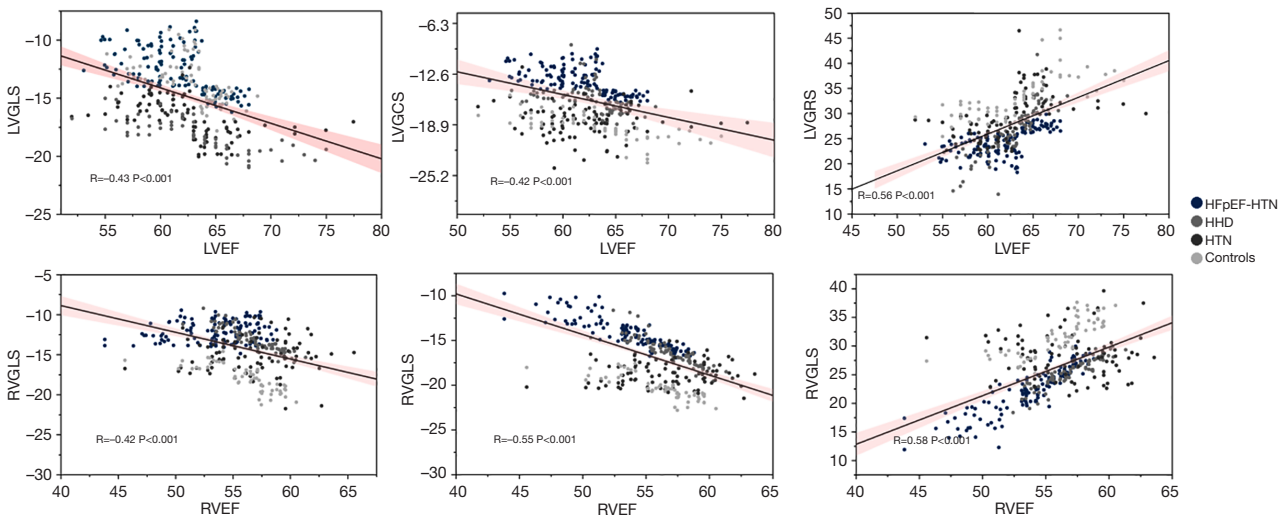

Figure 5 Correlations between myocardial strain parameters and LVEF and RVEF parameters. The pink shaded regions in the graph represent the 95% confidence intervals. LV, left ventricular; GLS, global longitudinal; LVEF, left ventricular ejection fraction; GCS, global circumferential strain; GRS, global radial strain; RV, right ventricular; RVEF, right ventricular ejection fraction; HFpEF, heart failure with preserved ejection fraction; HTN, hypertension; HHD, hypertensive heart disease.

Table 3 Logistic regression analysis with CMR parameters

Parameter	Univariate			Multivariate		
	OR	95% CI	P	OR	95% CI	P
LV GRS	0.848	0.780–0.922	<0.001	0.931	0.777–1.115	0.435
LV GCS	2.343	1.818–3.021	<0.001	1.681	1.149–2.459	0.007
LV GLS	1.262	1.085–1.468	0.003	0.82	0.513–1.310	0.406
RV GRS	0.747	0.671–0.831	<0.001	0.65	0.480–0.879	0.005
RV GCS	2.548	1.916–3.388	<0.001	2.614	1.504–4.542	<0.001
RV GLS	1.845	1.455–2.340	<0.001	4.617	2.005–10.630	<0.001
Native T1	1.017	1.012–1.022	<0.001	1.024	1.010–1.039	<0.001
ECV	1.579	1.396–1.825	<0.001	1.621	1.206–2.180	<0.001

CMR, cardiac magnetic resonance; OR, odds ratio; CI, confidence interval; LV, left ventricular; GRS, global radial strain; GCS, global circumferential strain; GLS, global longitudinal; RV, right ventricular; ECV, extracellular volume fraction.

exhibited a significantly higher ECV compared to controls. Furthermore, the study indicated that ECV reflects underlying changes in fibrosis, collagen expansion, and increased collagen cross-linking, all of which contribute to alterations in myocardial function. Other studies have confirmed a significant correlation between GLS and LVMi (r=0.42; P<0.002) and LVEF (r=–0.49; P<0.002) in patients with HTN. Moreover, recent research has demonstrated a linear relationship between LV GLS and log-transformed N-terminal pro b-BNP (26,27). Consistent with these findings, our study found there to be a moderate correlation of LV GLS and RV GLS with LVEF and RVEF, supporting the hypothesis that LV and RV strain parameters can offer valuable clinical insights in the assessment of cardiac dysfunction.

Our study also revealed significant differences in ECV and native T1 values between individuals with HTN and healthy controls, suggesting the presence of subtle cardiac

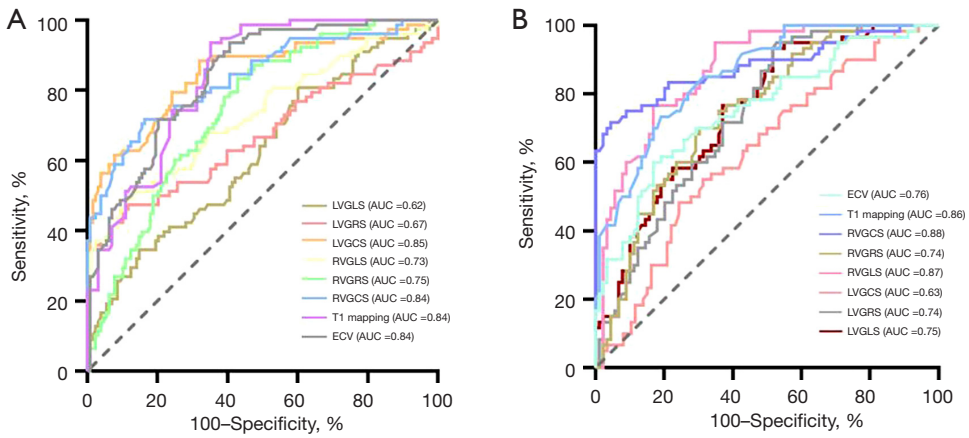

Figure 6 ROC curve analysis of feature tracking-derived LV and RV parameters for differentiating (A) HFpEF-HTN from HHD and (B) patients with HTN from healthy controls. LV, right ventricular; GLS, global longitudinal; AUC, area under the curve; GRS, global radial strain; GCS, global circumferential strain; RV, right ventricular; ECV, extracellular volume fraction; ROC, receiver operating characteristic; HFpEF, heart failure with preserved ejection fraction; HTN, hypertension; HHD, hypertensive heart disease.

Table 4 Intraobserver and interobserver myocardial strain and tissue characteristic parameters

Variable	Intraobserver		Interobserver	
	ICC	95% CI	ICC	95% CI
LV GRS (%)	0.981	0.961–0.995	0.980	0.972–0.989
LV GCS (%)	0.967	0.954–0.970	0.961	0.938–0.973
LV GLS (%)	0.967	0.957–0.981	0.937	0.912–0.968
RV GRS (%)	0.936	0.916–0.968	0.962	0.934–0.975
RV GCS (%)	0.968	0.951–0.981	0.982	0.969–0.990
RV GLS (%)	0.952	0.930–0.965	0.955	0.932–0.972
LGE percentages (%/LV)	0.962	0.942–0.972	0.960	0.942–0.977
Native T1 (ms)	0.924	0.913–0.937	0.925	0.917–0.942
ECV (%)	0.936	0.921–0.955	0.945	0.935–0.965

ICC, intraclass correlation coefficient; CI, confidence interval; LV, left ventricular; GRS, global radial strain; GCS, global circumferential strain; GLS, global longitudinal; RV, right ventricular; LGE, late gadolinium enhancement; ECV, extracellular volume fraction.

dysfunction in patients with HTN. This observation further implies that individuals with HTN may represent an intermediate stage between those with HFpEF-HTN and healthy controls. Previous research has indicated impaired GLS in patients with HTN-related LV hypertrophy who do not exhibit LGE despite maintaining preserved LVEF (28,29). Uncomplicated HTN could potentially initiate extracellular changes and myocardial fibrosis and thus may serve as an early mechanism in the progression from HTN to HHD and subsequently HF (30). Furthermore, despite valuable research efforts focused on HFpEF, a noninvasive and accurate diagnostic approach for HFpEF remains a challenge in clinical settings (31). Our study may provide novel insights into the identification of subtle systolic and diastolic dysfunction in individuals with HFpEF-HTN and into distinguishing HFpEF-HTN from HTN and HHD through use of noninvasive imaging parameters such as GLS, native T1 mapping, and ECV.

Limitations

It is important to acknowledge several limitations of

our study. To begin, the relatively small sample size from a single center might have restricted our ability to detect subtle associations. Additionally, since we used a retrospective design, our findings cannot be used for predictive purposes. Moreover, the body mass index (BMI) and gender distribution of individuals with HTN and healthy participants were not comparable; nonetheless, there were no significant differences observed between patients with HFpEF-HTN and those with HTN or HHD.

Conclusions

Myocardial strain, T1 mapping, and ECV may be feasibly used for the quantitative evaluation of LV and RV remodeling, dysfunction, and tissue characteristics in patients with HFpEF-HTN and thus have potential in the diagnosis of this condition.

Acknowledgments

This study was made possible by the wonderful work of colleagues in the Department of Radiology at The First Hospital of Lanzhou University.
Funding: The study was funded by The First Hospital of Lanzhou University (No. ldyyyn2023-99).

Footnote

Reporting Checklist: The authors have completed the STROBE reporting checklist. Available at https://qims.amegroups.com/article/view/10.21037/qims-24-803/rc

Conflicts of Interest: All authors have completed the ICMJE uniform disclosure form (available at https://qims.amegroups.com/article/view/10.21037/qims-24-803/coif). The authors have no conflicts of interest to declare.

Ethical Statement: The authors are accountable for all aspects of the work in ensuring that questions related to the accuracy or integrity of any part of the work are appropriately investigated and resolved. This study was conducted in accordance with the Declaration of Helsinki (as revised in 2013) and was approved by ethics committee of The First Hospital of Lanzhou University (No. LDYYLL-2024-470). The requirement for individual consent was waived due to the retrospective nature of the analysis.

References

1. Global, regional, and national age-sex specific mortality for 264 causes of death, 1980-2016: a systematic analysis for the Global Burden of Disease Study 2016. Lancet 2017;390:1151-210.
2. Yang G, Wang Y, Zeng Y, Gao GF, Liang X, Zhou M, Wan X, Yu S, Jiang Y, Naghavi M, Vos T, Wang H, Lopez AD, Murray CJ. Rapid health transition in China, 1990-2010: findings from the Global Burden of Disease Study 2010. Lancet 2013;381:1987-2015.
3. Global, regional, and national under-5 mortality, adult mortality, age-specific mortality, and life expectancy, 1970-2016: a systematic analysis for the Global Burden of Disease Study 2016. Lancet 2017;390:1084-150.
4. Wang Z, Chen Z, Zhang L, Wang X, Hao G, Zhang Z, Shao L, Tian Y, Dong Y, Zheng C, Wang J, Zhu M, Weintraub WS, Gao R; China Hypertension Survey Investigators. Status of Hypertension in China: Results From the China Hypertension Survey, 2012-2015. Circulation 2018;137:2344-56.
5. Donal E, Lund LH, Oger E, Hage C, Persson H, Reynaud A, Ennezat PV, Bauer F, Sportouch-Dukhan C, Drouet E, Daubert JC, Linde C; KaRen Investigators. Baseline characteristics of patients with heart failure and preserved ejection fraction included in the Karolinska Rennes (KaRen) study. Arch Cardiovasc Dis 2014;107:112-21.
6. Lam CS, Donal E, Kraigher-Krainer E, Vasan RS. Epidemiology and clinical course of heart failure with preserved ejection fraction. Eur J Heart Fail 2011;13:18-28.
7. He J, Sirajuddin A, Li S, Zhuang B, Xu J, Zhou D, Wu W, Sun X, Fan X, Ji K, Chen L, Zhao S, Arai AE, Lu M. Heart Failure With Preserved Ejection Fraction in Hypertension Patients: A Myocardial MR Strain Study. J Magn Reson Imaging 2021;53:527-39.
8. Rademakers FE. Magnetic resonance imaging in

cardiology. Lancet 2003;361:359-60.
9. Claus P, Omar AMS, Pedrizzetti G, Sengupta PP, Nagel E. Tissue Tracking Technology for Assessing Cardiac Mechanics: Principles, Normal Values, and Clinical Applications. JACC Cardiovasc Imaging 2015;8:1444-60.
10. He J, Yang W, Wu W, Sun X, Li S, Yin G, Zhuang B, Xu J, Zhou D, Zhang Y, Wang Y, Zhu L, Sharma P, Sirajuddin A, Teng Z, Kureshi F, Zhao S, Lu M. Clinical features, myocardial strain and tissue characteristics of heart failure with preserved ejection fraction in patients with obesity: A prospective cohort study. EClinicalMedicine 2023;55:101723.
11. Pieske B, Tschöpe C, de Boer RA, Fraser AG, Anker SD, Donal E, et al. How to diagnose heart failure with preserved ejection fraction: the HFA-PEFF diagnostic algorithm: a consensus recommendation from the Heart Failure Association (HFA) of the European Society of Cardiology (ESC). Eur J Heart Fail 2020;22:391-412.
12. Salton CJ, Chuang ML, O'Donnell CJ, Kupka MJ, Larson MG, Kissinger KV, Edelman RR, Levy D, Manning WJ. Gender differences and normal left ventricular anatomy in an adult population free of hypertension. A cardiovascular magnetic resonance study of the Framingham Heart Study Offspring cohort. J Am Coll Cardiol 2002;39:1055-60.
13. Le TT, Tan RS, De Deyn M, Goh EP, Han Y, Leong BR, Cook SA, Chin CW. Cardiovascular magnetic resonance reference ranges for the heart and aorta in Chinese at 3T. J Cardiovasc Magn Reson 2016;18:21.
14. Olivotto I, Maron MS, Autore C, Lesser JR, Rega L, Casolo G, De Santis M, Quarta G, Nistri S, Cecchi F, Salton CJ, Udelson JE, Manning WJ, Maron BJ. Assessment and significance of left ventricular mass by cardiovascular magnetic resonance in hypertrophic cardiomyopathy. J Am Coll Cardiol 2008;52:559-66.
15. Unger T, Borghi C, Charchar F, Khan NA, Poulter NR, Prabhakaran D, Ramirez A, Schlaich M, Stergiou GS, Tomaszewski M, Wainford RD, Williams B, Schutte AE. 2020 International Society of Hypertension Global Hypertension Practice Guidelines. Hypertension 2020;75:1334-57.
16. Messroghli DR, Greiser A, Fröhlich M, Dietz R, Schulz-Menger J. Optimization and validation of a fully-integrated pulse sequence for modified look-locker inversion-recovery (MOLLI) T1 mapping of the heart. J Magn Reson Imaging 2007;26:1081-6.
17. Li H, Zheng Y, Peng X, Liu H, Li Y, Tian Z, Hou Y, Jin S, Huo H, Liu T. Heart failure with preserved ejection fraction in post myocardial infarction patients: a myocardial magnetic resonance (MR) tissue tracking study. Quant Imaging Med Surg 2023;13:1723-39.
18. Mills KT, Stefanescu A, He J. The global epidemiology of hypertension. Nat Rev Nephrol 2020;16:223-37.
19. Triposkiadis F, Sarafidis P, Briasoulis A, Magouliotis DE, Athanasiou T, Skoularigis J, Xanthopoulos A. Hypertensive Heart Failure. J Clin Med 2023;12:5090.
20. Pieske B, Tschöpe C, de Boer RA, Fraser AG, Anker SD, Donal E, et al. How to diagnose heart failure with preserved ejection fraction: the HFA-PEFF diagnostic algorithm: a consensus recommendation from the Heart Failure Association (HFA) of the European Society of Cardiology (ESC). Eur Heart J 2019;40:3297-317.
21. Authors/Task Force Members: McDonagh TA, Metra M, Adamo M, Gardner RS, Baumbach A, Böhm M, et al. 2023 Focused Update of the 2021 ESC Guidelines for the diagnosis and treatment of acute and chronic heart failure: Developed by the task force for the diagnosis and treatment of acute and chronic heart failure of the European Society of Cardiology (ESC) With the special contribution of the Heart Failure Association (HFA) of the ESC. Eur J Heart Fail 2024;26:5-17.
22. He J, Yang W, Wu W, Li S, Yin G, Zhuang B, Xu J, Sun X, Zhou D, Wei B, Sirajuddin A, Teng Z, Zhao S, Kureshi F, Lu M. Early Diastolic Longitudinal Strain Rate at MRI and Outcomes in Heart Failure with Preserved Ejection Fraction. Radiology 2021;301:582-92.
23. Santos AB, Roca GQ, Claggett B, Sweitzer NK, Shah SJ, Anand IS, Fang JC, Zile MR, Pitt B, Solomon SD, Shah AM. Prognostic Relevance of Left Atrial Dysfunction in Heart Failure With Preserved Ejection Fraction. Circ Heart Fail 2016;9:e002763.
24. van Veldhuisen DJ, Linssen GC, Jaarsma T, van Gilst WH, Hoes AW, Tijssen JG, Paulus WJ, Voors AA, Hillege HL. B-type natriuretic peptide and prognosis in heart failure patients with preserved and reduced ejection fraction. J Am Coll Cardiol 2013;61:1498-506.
25. Mordi IR, Singh S, Rudd A, Srinivasan J, Frenneaux M, Tzemos N, Dawson DK. Comprehensive Echocardiographic and Cardiac Magnetic Resonance Evaluation Differentiates Among Heart Failure With Preserved Ejection Fraction Patients, Hypertensive Patients, and Healthy Control Subjects. JACC Cardiovasc Imaging 2018;11:577-85.
26. Neisius U, Myerson L, Fahmy AS, Nakamori S, El-Rewaidy H, Joshi G, Duan C, Manning WJ, Nezafat R. Cardiovascular magnetic resonance feature tracking strain analysis for discrimination between hypertensive heart

disease and hypertrophic cardiomyopathy. PLoS One 2019;14:e0221061.
27. DeVore AD, McNulty S, Alenezi F, Ersboll M, Vader JM, Oh JK, Lin G, Redfield MM, Lewis G, Semigran MJ, Anstrom KJ, Hernandez AF, Velazquez EJ. Impaired left ventricular global longitudinal strain in patients with heart failure with preserved ejection fraction: insights from the RELAX trial. Eur J Heart Fail 2017;19:893-900.
28. Niu J, Zeng M, Wang Y, Liu J, Li H, Wang S, Zhou X, Wang J, Li Y, Hou F, Zhu J. Sensitive marker for evaluation of hypertensive heart disease: extracellular volume and myocardial strain. BMC Cardiovasc Disord 2020;20:292.
29. Liu H, Wang J, Pan Y, Ge Y, Guo Z, Zhao S. Early and Quantitative Assessment of Myocardial Deformation in Essential Hypertension Patients by Using Cardiovascular Magnetic Resonance Feature Tracking. Sci Rep 2020;10:3582.
30. Ekström M, Hellman A, Hasselström J, Hage C, Kahan T, Ugander M, Wallén H, Persson H, Linde C. The transition from hypertension to hypertensive heart disease and heart failure: the PREFERS Hypertension study. ESC Heart Fail 2020;7:737-46.
31. Wen J, Zhang X, Li S, Tao X, Fang Q, Zhou S, Xia L, Gong L. Identification of heart failure with preserved ejection fraction in patients with hypertension: a left atrial myocardial strain cardiac magnetic resonance study. Quant Imaging Med Surg 2023;13:2881-94.

Cite this article as: Li R, Lei F, Liu F, Cao L, Cao X, Niu M, Guo S. The transition from hypertension to hypertensive heart disease and heart failure with preserved ejection fraction: a retrospective cross-sectional study of myocardial magnetic resonance strain and tissue characteristics. Quant Imaging Med Surg 2024;14(10):7684-7696. doi: 10.21037/qims-24-803

